Songklanakarin J. Sci. Technol.
33 (1), 69-78, Jan. - Feb. 2011

SJST SONGKLANAKARIN JOURNAL OF SCIENCE AND TECHNOLOGY
http://www.sjst.psu.ac.th

Original Article

A novel linear switched reluctance motor : Investigation and experimental verification

Natesan Chokkalingam Lenin[1]*, Rengasamy Arumugam[2] and Member IEEE

[1] *Department of Electrical Engineering, St. Joseph's College of Engineering, Chennai, India.*

[2] *Department of Electrical Engineering, SSN College of Engineering, Chennai, India.*

Received 6 June 2010; Accepted 20 February 2011

Abstract

A novel stator geometry for a linear switched reluctance motor (LSRM) that improves the force profile is presented in this paper. In the new geometry, pole shoes are affixed on the stator poles. Static characteristics for the proposed structure have been highlighted using two dimensional (2-D) finite element analyses (FEA). A detailed sensitivity analysis of the effect of several geometrical parameters on the performance of the proposed LSRM is presented. Further, motor performance for variable load conditions is discussed. The 2-D FEA results and the experimental results of this paper prove that LSRMs are one of the strong candidates for linear propulsion drives.

Keywords: linear switched reluctance motor, finite element analysis, sensitivity analysis. .

1. Introduction

Linear switched reluctance motors (LSRMs) are an attractive alternative to linear induction or synchronous machines due to lack of windings on the stator or translator structure, easier manufacturing and maintenance, good fault tolerance capability (Miller, 1993). LSRMs are classified as (a) longitudinal flux and (b) transverse flux. This paper is dedicated to the longitudinal flux LSRM. A design procedure for longitudinal-flux LSRM has been described in Byeong-Seok *et al.* (2000). Other types of longitudinal-flux LSRMs are presented in Chayopitak *et al.* (2005), with coupled flux paths, and in Sun *et al.* (2008) with uncoupled flux paths for a magnetic levitation system. A high force longitudinal-flux double-sided double-translator LSRM has been analysed in Deshpande *et al.* (1995). Longitudinal-flux LSRMs have been proposed for applications such as precise motion control Pan *et al.* (2005); Zhao *et al.* (2007) and as propulsion systems for railway vehicles Kolomeitsev *et al.* (2008) or vertical elevators Lim *et al.* (2007); Lobo *et al.* (2008).

The sensitivity of geometry in the performance of rotating SRMs has been extensively described in the literature Arumugam *et al.* (1988); Sheth *et al.* (2003). The sensitivity of pole arcs on average torque is studied using an analytical method and 2-D finite-element analysis (2-D FEA) in Arumugam *et al.* (1988). In Faiz *et al.* (1993), the sensitivity analysis is conducted by means of an analytical model based on air-gap permeance and the equivalent magnetic circuit. Murthy *et al.* (1998) studies the sensitivity of pole arcs and air-gap length on the average torque using 2-D FEA. In Sheth *et al.* (2003), the sensitivity of the stator and rotor pole arcs is studied to minimize torque ripple. Up to now, very little has been published on the sensitivity of geometrical parameters in LSRM performance. However, it is important to mention the work presented in Liu *et al.* (1999) on the feasible stator- and translator-pole arrangements in longitudinal- and trans-

* Corresponding author.
Email address: nclenin@gmail.com

verse-flux LSRMs. This paper intends to address how several geometrical parameters influence the inductance and force profile of a longitudinal flux LSRM.

Despite of the various advantages, LSRMs has some drawbacks such as high force ripple, vibration, acoustic noise and need of power electronic converters. Several efforts to reduce or eliminate the torque ripple of the rotary switched reluctance motors (RSRMs) have been presented in the literature Schramm *et al.* (1992); Neagoe *et al.* (1997). Multi phase excitation to reduce the force ripple in the LSRM has been explained in Han-Kyung Bae *et al.* (2000). However, the previous method considerably increases the copper losses. In this paper a novel stator structure for a longitudinal flux LSRM is proposed to reduce the force ripple. Two dimensional (2D) finite element analysis (FEA) is carried out to predict the performance of the conventional and the proposed structures.

The organization of the paper is as follows: Section II presents new stator geometry for LSRMs that improves the force profile and FEA results for the conventional and the proposed structures. Section III presents the sensitivity analysis of the geometrical parameters. Section IV contains motor performance for variable load conditions. Experimental results from the prototype machine and their correlation with FEA results are presented in Section V. Conclusions and future work are summarized in Section VI.

2. Force Ripple Analysis Using An Alternative Geometry

2.1 Definition, Sources of the force ripple and techniques to reduce it

Assuming that the maximum value of the static force as F_{max}, the minimum value that occurs at the intersection point of two consecutive phases as F_{min}, and the average force as F_{avg}, the percentage force ripple may be defined as (1)

$$\%Force\ Ripple = \frac{F_{max} - F_{min}}{F_{avg}} \times 100 \quad (1)$$

The causes of the force ripple in LSRMs are mainly due to the switching of phase currents into its windings and the highly nonlinear nature of the phase inductance variation when the translator moves. These force pulsations contribute to vibrations and acoustic noise in LSRMs.There are two approaches to force profile improvement. One approach is to suitably shape the input excitation current profile by using an electronic control of the power controllers. The second approach is to modify the geometry of the poles of the stator and translator. This research makes an attempt to examine the force profile by the geometry modifications approach, by providing pole shoes on the stator poles.

2.2 Effect of stator pole shaping on the force profile

This sensitivity study aims mainly to determine the improvement in the force profile when the stator pole width gets varied. The conventional LSRM which is considered in this paper is shown in Figure 1(a). The specifications of the conventional machine are given in Table 1.

The width of the stator pole is varied from 16 mm to 21 mm in steps. The translator geometry remains unchanged throughout the sensitivity study. The height of the stator pole is fixed. The field analysis has been carried out for a phase excitation of 10 A. The predicted propulsion force, normal force, inductance profiles and average force are shown in Figure 1(b). Table 2 summarizes the comparison of the studied configurations.

From Table 2 it can be observed that, when the stator pole width is increased, there is a reduction in the average force, which is not large after a certain point. Figure 1(b) to (d) show the stator pole length/pole pitch versus average force. From that, we inferred the maximum average force and the low force ripple occurs, when the pole width is 19 mm.

2.3 force ripple minimization using stator pole shoes

In this section, improving the force profile using stator pole shoes is investigated by a 2-D finite-element analysis. The difference between the conventional and the proposed stator poles are shown in Figure 2. The cross sectional view of the proposed LSRM with pole shoes is shown in Figure 3(a).

The aim in proposing the stator pole shoe is to widen the stator pole width to smoothen the force profile. The analysis is carried out on the conventional LSRM with a pole

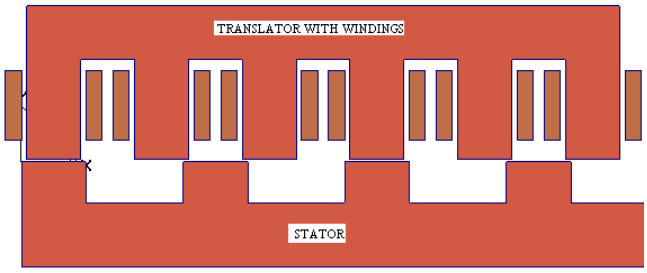

Figure 1 (a). 2D cross sectional view of the conventional LSRM.

Table 1. Specifications and dimensions of the studied LSRM

l_g = 1.5 mm	w_{sp} = 21 mm
F_{max} = 120 N	h_{sp} = 30 mm
L_{stack} = 40 mm	w_{sy} = 35mm
Steel type (Stator) - M 45	w_{ss} = 31 mm
Steel type (Translator) - M 45	w_{ts} = 26 mm
Travel length= 2 m	h_{tp} = 48 mm
V_{rated} = 120 V	w_{tp} = 13 mm
I_{rated} = 10 A	w_{ty} = 30mm
N_{ph} = 396	Wire size = AWG 18

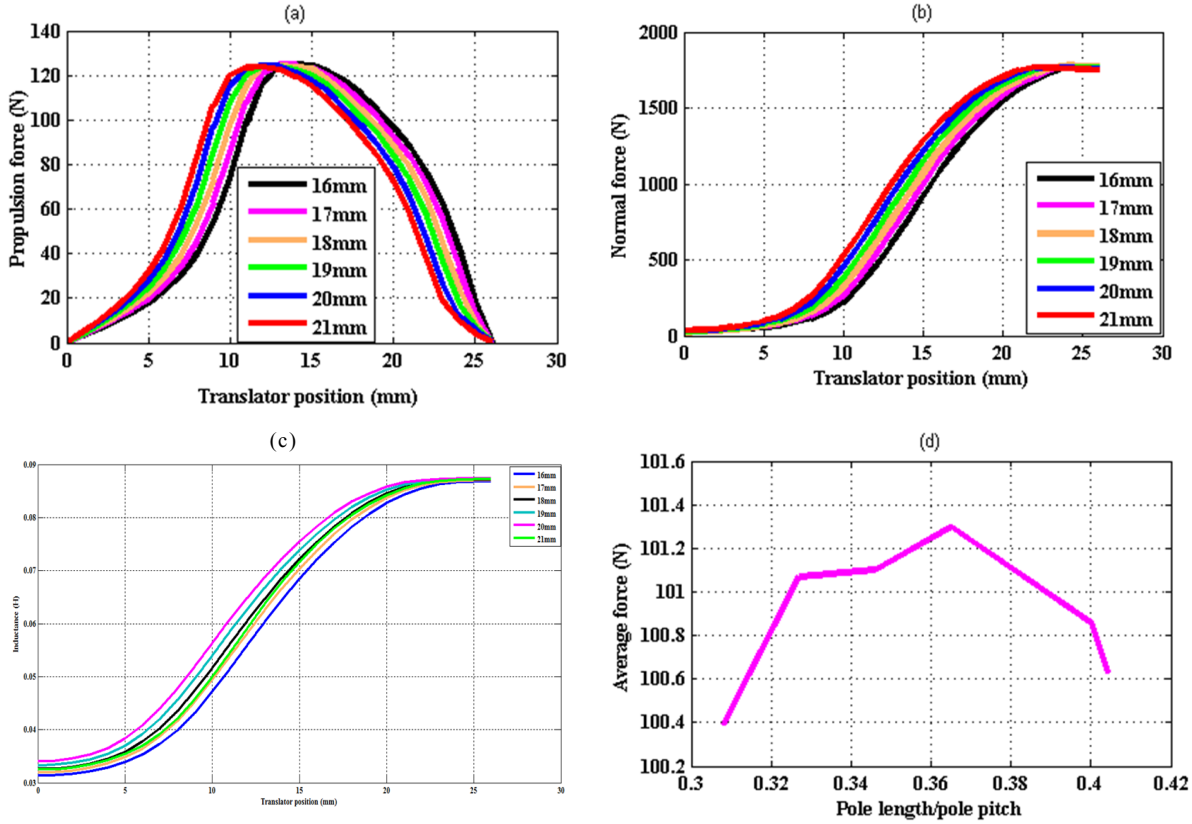

Figure 1(b). Force and Inductance for various stator pole widths (without pole shoes).

Table 2. Comparison of force ripple for various stator pole widths (without pole shoes)

W_{sp} (mm)	F_{min} (N)	F_{max} (N)	F_{avg} (N)	% ripple	L_{min} (H)	L_{max} (H)
16	67.33	124.87	100.39	60.38	0.02972	0.08626
17	67.91	124.70	101.07	57.68	0.03019	0.08658
18	68.23	124.57	101.10	55.88	0.03071	0.08683
19	68.32	124.11	101.30	53.41	0.03125	0.087
20	68.28	124.34	100.86	56.16	0.03184	0.08713
21	67.88	123.90	100.63	55.67	0.03246	0.08725

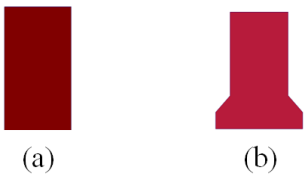

Figure2. (a) Conventional (b) Proposed

shoe, which is affixed on the stator poles. The width of the stator pole shoe is 4 mm. The stator pole width is varied from 16mm to 20 mm in steps. The width of the pole shoe and overall height of the stator pole are maintained constant. The mutual inductance and leakage effects are neglected. The simulation is presented for an excitation current of 10 A.

The predicted propulsion force, normal force, inductance profiles and the average force are shown in Figure 3(b). Table 3 summarizes the comparison of the studied configureurations with pole shoes. Figure 3(b) to (d) shows the stator pole length/pole pitch versus average force. From that, the maximum average force occurs when the stator pole width is 19 mm with a 4 mm pole shoe.

2.4 Discussion on 2-D FEA Results

This section addresses an important technical problem in LSRMs, specifically the force ripple. A study of the same by modifying the stator pole and affixing stator pole

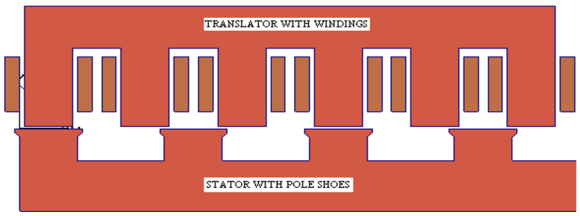

Figure 3(a). 2D cross sectional view of the proposed LSRM.

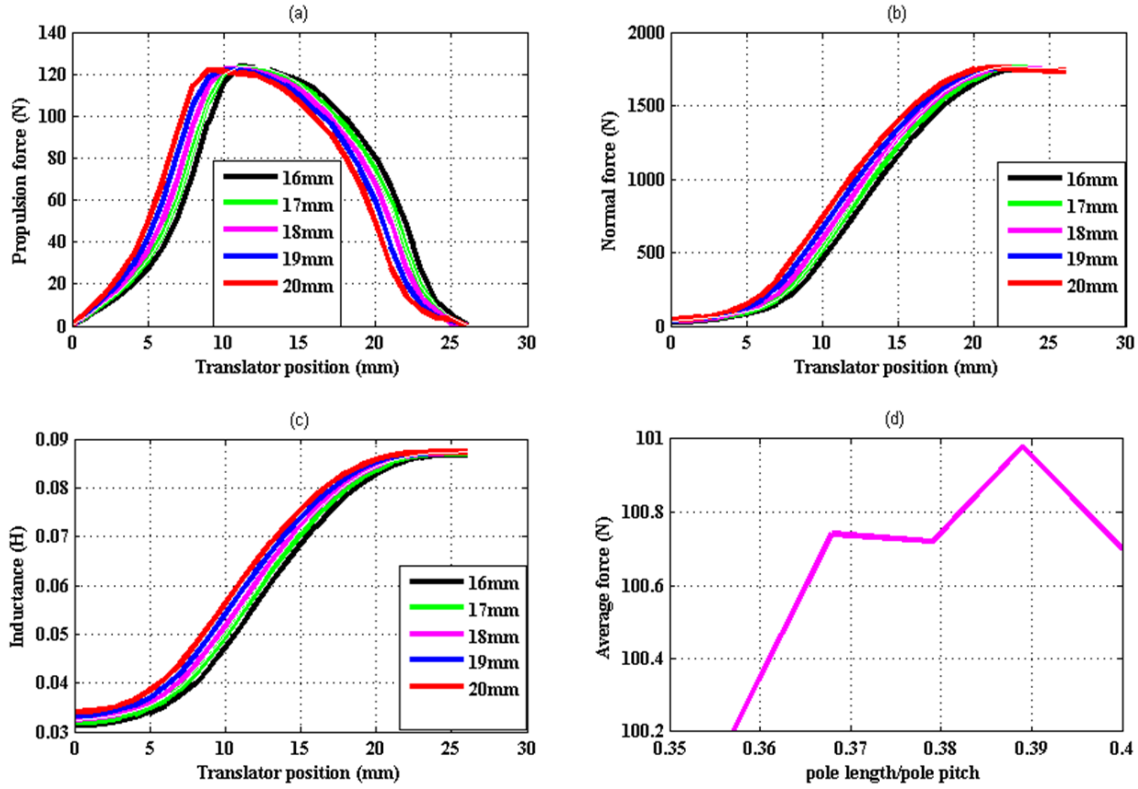

Figure 3(b). Force and Inductance for various stator pole widths (with pole shoes).

shoes and the observations made from the 2-D FEA used for field simulation results on this geometry are reported. The provision of stator pole shoes improves the force profile and reduces the force ripple at the maximum force regions. Hence, the maximum force is allowed to remain the same for more positions of the translator. The extent of the low force region around the unaligned position is reduced due to the addition of pole shoes. From Table 3 it can be observed that, as the stator pole width is increased, keeping the stator pole shoe width as constant, there is a reduction in the average force, which is not large after a certain point. The sensitivity study also depicts that any reduction in the width of the stator pole for the same variations of the pole shoe arcs, contributes to a loss of the average force. It is generally accepted that decreasing the stator pole width will decrease the aligned inductance with negligible effect on the unaligned inductance. This is reflected in Table 2 obtained from a 2-D FEA field simulation. Finally, the stator volume, stator mass and the %- force ripple reduction are compared in Table 4. From Table 4 we inferred that, the proposed LSRM (19 mm stator pole width) has high force density, less force ripple and volume when compared to the conventional machine. So, for the other analysis in this paper we prefer LSRM with pole shoe having 19 mm pole width.

3. Sensitivity Analysis

3.1 influence of pole heights

3.1.1 Stator pole height

In this part of the analysis, the variables are stator pole height and the translator position. The other geometrical parameters are kept constant as shown in Table 1. The current density is 4.86 A/mm^2. The results are shown in Figure 4(a) and it is evident that, a longer pole length means a

Table 3. Comparison of force ripple for various stator pole widths (with pole shoes)

W_{sp} (mm)	F_{min} (N)	F_{max} (N)	F_{avg} (N)	% ripple	L_{min} (H)	L_{max} (H)
16	69.30	123.33	100.2	53.97	0.03130	0.08681
17	68.83	122.76	100.74	53.54	0.03194	0.08708
18	68.84	122.18	100.72	52.95	0.03260	0.08723
19	68.62	121.78	100.98	52.64	0.03327	0.08730
20	68.27	121.77	100.70	53.12	0.03403	0.08737

Table 4. Comparison of volume, mass and force ripple

W_{sp} (mm)	Volume (m^3)		Mass (kg)		Force ripple reduction (%)
	Without pole shoes	With pole shoes	Without pole shoes	With pole shoes	
16	0.00243	0.00238	18.68	18.37	10.62
17	0.00245	0.00242	18.88	18.64	7.18
18	0.00247	0.00245	19.10	18.92	5.24
19	0.00250	0.00249	19.28	19.19	1.44
20	0.00253	0.00252	19.48	19.46	5.41
21	0.00255	NA	19.67	NA	NA

NA: not analysed in this paper.

higher peak and average force.

3.1.2 Translator pole height

In this part of the analysis, the variables are translator pole height and the translator position. The other geometrical parameters are kept constant as shown in Table 1. The current density is 4.86 A /mm^2. The results are shown in Figure 4(b). From the Figure 4(b) (i), the influence of the translator pole length is significant for values of translator pole length lower than 48 mm. Above this value; there is no influence on average force which is evident from Figure 4(b) (ii).

3.2 Influence of stack length

In this part of the analysis, the variables are stack length and the translator position. The other geometrical parameters are kept constant as shown in Table 1. The current density is 4.86 A/mm^2. The stack length is varied from 20mm to 100mm. Figure 4(c) (i) shows the sensitivity of stack length on force profiles. Figure 4(c) (ii) shows the sensitivity of stack length on the average force for several current densities. From that, it is evident that the average force increases linearly with the stack length.

3.3 Influence of air-gap length

In LSRMs, the air gap does not condition any other dimension. The variables in this part of the analysis are air gap length and the translator position. The other geometrical parameters are kept constant as shown in Table 1. The current density is 4.86 A /mm^2. The air gap length is varied from 0.3 mm to 2 mm. Figure 4(d) (i) shows the sensitivity of the force profiles on the air gap length. The sensitivity of air gap length on the average force can be seen in Figure 4(d) (ii). From that, the smaller the air gap, higher the average force.

3.4 Influence of translator pole width

The variables in this part of the analysis are translator pole width and the translator position. The other geometrical parameters are kept constant as shown in Table 1. The current density is 4.86 A/mm^2. The translator pole width is increased from 8 mm to 15 mm. Figure 4(e) (i) shows the sensitivity of force profiles on the translator pole width. The sensitivity of translator pole width on the average force can be seen in Figure 4(e) (ii). From that, the average force is increasing linearly with the translator pole width. However, increasing the pole width proportionally increases the mass of the translator.

3.5 Influence of pole shoe width

In this part of the analysis, the variables are pole shoe width and the translator position. The other geometrical parameters are kept constant as shown in Table 1. The current density is 4.86 A/mm^2. The pole shoe width is varied from 1mm to 6mm in steps. Figure 4(f) (i) shows the sensi-

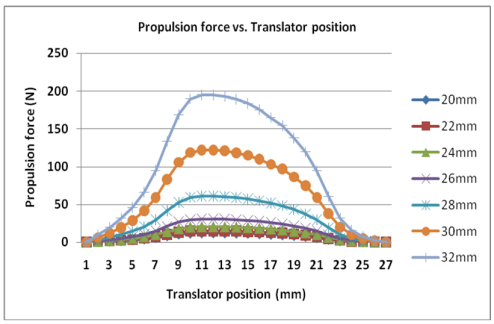

a. Sensitivity of stator pole height

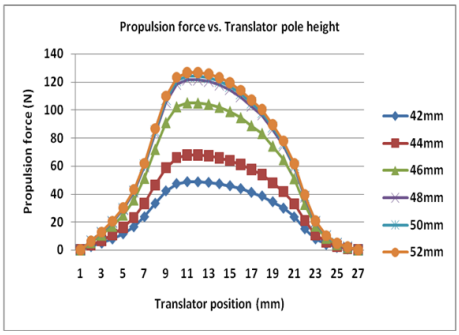

(1)

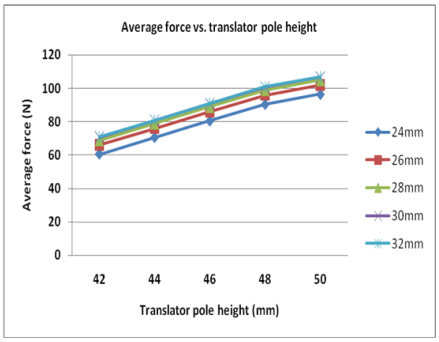

(2)

b. Sensitivity of translator pole height

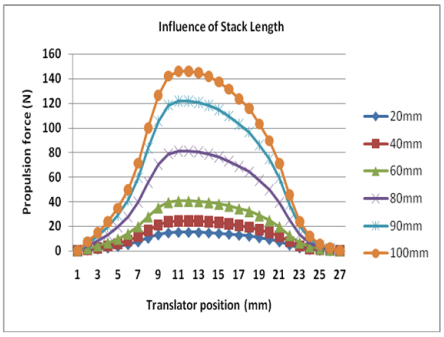

(1)

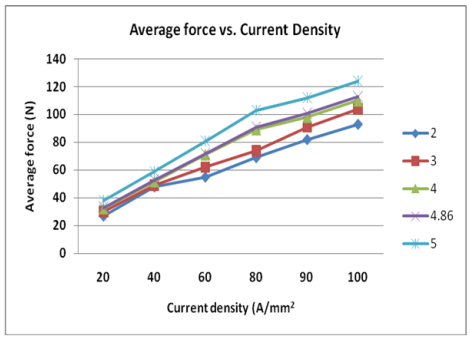

(2)

c. Sensitivity of stack length

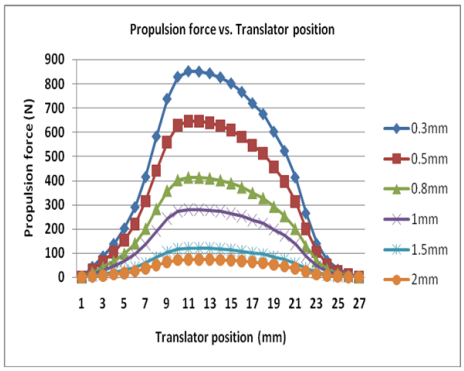

(1)

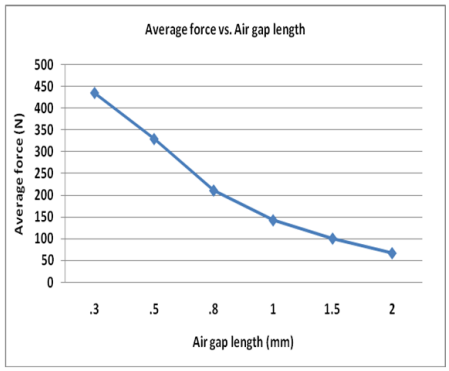

(2)

d. Sensitivity of air gap length

Figure 4. Sensitivity of geometrical parameters for the proposed structure.

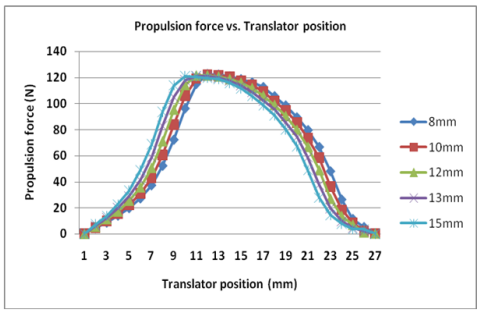

(1)

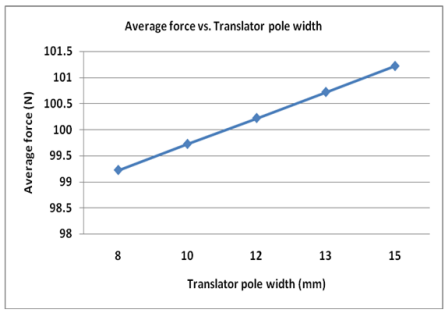

(2)

e. Sensitivity of translator pole width

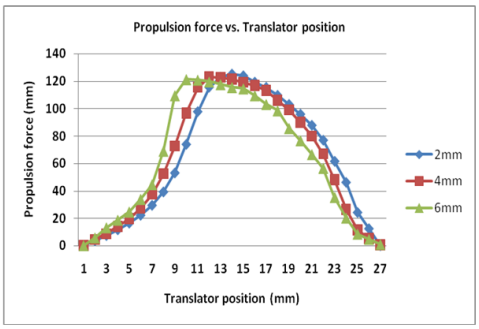

(1)

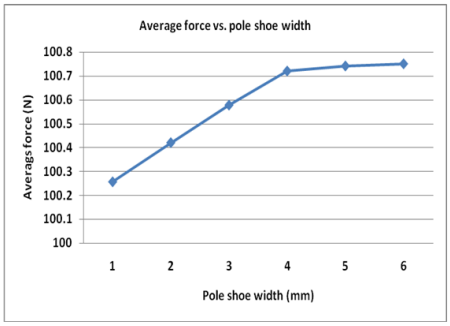

(2)

f. Sensitivity of pole shoe width

Figure 4. (Continued)

tivity of pole shoe width on force profiles only for three pole widths. Figure 4(f) (ii) shows the sensitivity of pole shoe width on the average force. From that, the average force increases linearly with the pole shoe width up to 4 mm. After that, there will no significant change in the average force.

4. Motor Performance For Variable Load Conditions

In practice, motors operate with changing load conditions. The influence of load variation on some of the parameters like the velocity, current, and the efficiency of the motor are studied. The results shown in Table 5 are obtained when the circuit is turned ON at the point when the inductance starts to increase and turned OFF before it starts to decrease.

Figure5 (a) shows the velocity and current variation for different load conditions. The velocity steadily decreases with an increase in load. This characteristic reminds of the speed-load characteristic of a series DC motor. Figure5 (b) shows the characteristics of mechanical power P_m, and the efficiency with change in load. It can be seen that, initially as the load increases the efficiency increases and when load is further increased the efficiency started to decrease. Figure 5 (c) shows the characteristics of the efficiency with change in mechanical power P_m. It can be seen that, the efficiency is high at most cases, encouraging the proposal of the pole shoe concept in LSRM.

5. Experimental Results

Figure 6 shows the actual experimental setup for the prototype LSRM with the stator pole shoe that is used as a material carrying vehicle in the laboratory. The experimental road is 2 m long and translator weight is 12 kg. It should be noted that the present setup is intended for development purposes only. Figure 7 shows actual phase voltage and phase current waveforms of the LSRM.

6. Conclusion

A modification of the stator geometry by the provision of stator pole shoes has been presented. A prototype LSRMs is modeled, simulated, analyzed, developed, and experimentally validated with the conventional control strategy. The following conclusions are observed when compared to the conventional machine: (a) Force ripple is reduced by 5.44% , (b) Volume of the stator is reduced by 2.35%, (c) mass of the stator is reduced by 2.44%, (d) Force density is high in the proposed structure, (e) Sensitivity analysis of several geometrical parameters helps the designer

Table 5. Influence of load on motor performance

F_L (N)	I (A)	V (m/s)	Input power (W)	Output power (W)	Efficiency (%)
2	2.09	10.42	57.85	26.12	45.15
5	3.28	8.03	65.84	31.46	47.78
10	4.72	6.40	91.39	39	42.67
20	5.31	4.02	114.61	46.99	41
40	6.19	3.35	151.36	57.70	38.12
60	7.87	2.65	181.32	63.66	35.11
80	8.29	1.28	196.36	67	34.12
100	9.79	0.5	214.45	71.11	33.16
120	10.5	0.15	255.84	77.8	30.41

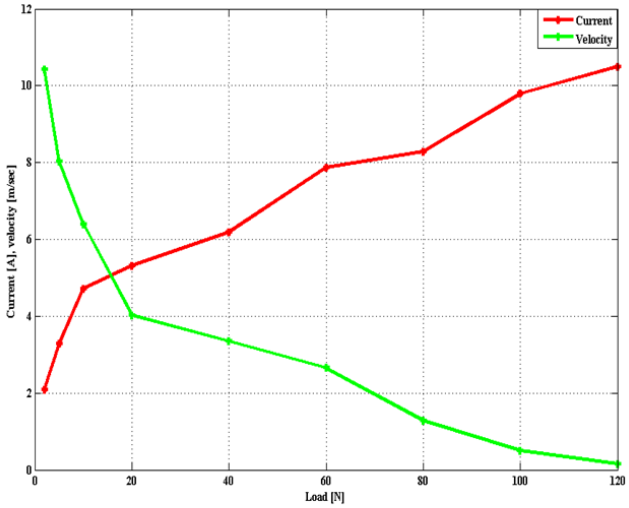

(a)

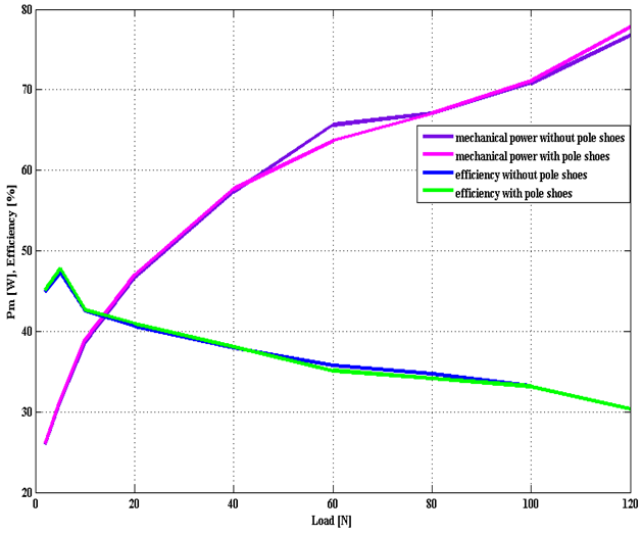

(b)

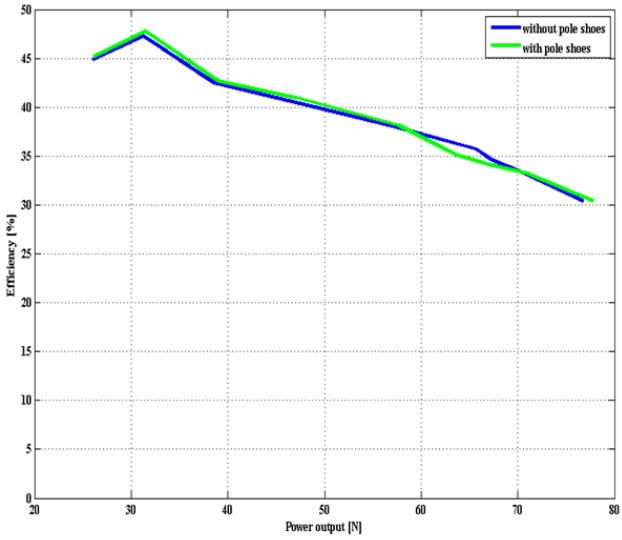

(c)

Figure 5. (a) Variation of current and velocity with load, (b) variation of P_m, efficiency with load, and (c) variation of efficiency with P_m.

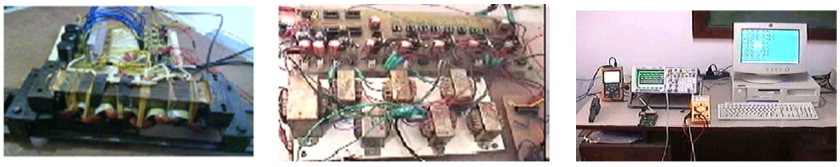

(a) (b) (c)

Figure 6. Experimental setup of (a) LSRM and converter, (b) driver circuit, and (c) PC along with measuring instruments.

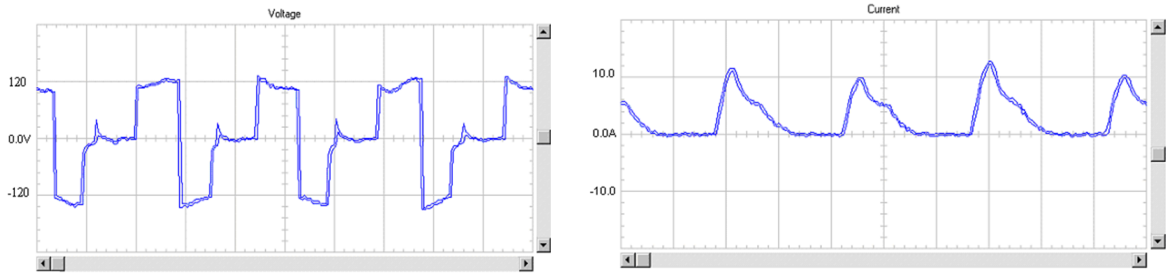

(a) (b)

Figure 7. Experimental waveforms during single pulse operation: (a) Actual phase voltage of LSRM, and (b) Actual phase current of LSRM.

to optimize the design variables according to the applications, (f) The maximum efficiency occures at a load force of 5N, which is also high when compared to the conventional LSRM, and (g) There is a good agreement between measurement results and FEA values of the inductance profile.

The proposed stator pole shoe geometry research can be further extended to study the thermal, stress, and vibration analyses.

References

Arumugam, R., Lindsay, J. F., and Krishnan, R. 1988. Sensitivity of pole arc/pole pitch ratio on switched reluctance motor performance, vol. 1, pp. 50-54.

Bae, H K, Lee, B. S., Vijayaraghavan, P, and Krishnan, R. 2000. A linear switched reluctance motor: Converter and Control, IEEE Transactions on Industry Applications, 36(5), 1351-1359.

Byeong-Seok, L., Han-Kyung, B., Praveen, V., and Krishnan, R. 2000. Design of a linear switched reluctance machine, IEEE Trans. Ind. Appl., 36(6), 1571-1580.

Chayopitak, N., and Taylor, D. G. 2005. Design of linear variable reluctance motor using computer-aided design assistant, *Proc*. IEEE Int. Conf. Elect. Mach. Drives, May 2005, 1569-1575.

Deshpande, U. S., Cathey, J. J., and Richter, E. 1995. High-force density linear switched reluctance machine, IEEE Trans. Ind. Appl., 31(2), 345-352.

Faiz, J., and Finch, J. W. 1993. Aspects of design optimization for switched reluctance motors, IEEE Trans. Energy Convers., 8(4), 704-713.

Iqbal Hussain and Ehsani, M. 1996. Torque Ripple Minimization in Switched Reluctance Motor Drives by PWM Current Control, IEEE Trans., on Power Electronics, 11(1), 83-88.

Kolomeitsev, L., Kraynov, D., Pakhomin, F., Rednov, F., Kallenbach, E., Kireev, V., Schneider, T., and Böcker, J. 2008. Linear switched reluctance motor as high efficiency propulsion system for railway vehicles, Proc. SPEEDAM, 2008, 155-160.

Lim, H. S., and Krishnan, R. 2007. Ropeless elevator with linear switched reluctance motor drive actuation systems, IEEE Trans. Ind. Electron., 54(4), 2209-2218.

Lim, H. S., Krishnan, R., and Lobo, N. S. 2008. Design and control of a linear propulsion system for an elevator using linear switched reluctance motor drives, IEEE Trans. Ind. Electron., 55(2), 534-542.

Liu, C. T., and Chen, Y.-N. 1999. On the feasible polygon classification of linear switched reluctance machines, IEEE Trans. Energy Convers., 14(4), 1282-1287.

Lobo, N. S., Lim, H. S., and Krishnan, R. 2008. Comparison of linear switched reluctance machines for vertical propulsion application: Analysis, design, and experimental correlation, IEEE Trans. Ind. Appl., 44(4), 1134-1142.

Miller, T.J.E. 1993. Switched Reluctance Motor and Their Control. Hillsboro, OH: Magna Phys.

Moallem, M., Ong, C. M., and Unnewehr, L. E. 1992. Effect of rotor profiles on the torque of a switched reluctance motor, IEEE Trans. on Ind. Applicat., 28(2), 364-369.

Murthy, S. S., Singh, B., and Sharma, V. K. 1998. Finite element analysis to achieve optimum geometry of switched

reluctance motor, Proc. IEEE TENCON, 1998, 2, 414-418.

Neagoe, C., Foggia, A., and Krishnan, R. 1997. Impact of pole tapering on the electromagnetic force of the switched reluctance motor, Conf. Rec. IEEE Electric Machines and Drives Conference, 1997, WA1/2.1- WA1/2.3.

Pan, J., Cheung, N. C., and Yang, J. 2005. High-precision position control of a novel planar switched reluctance motor, IEEE Trans. Ind. Electron., 52(6), 1644-1652.

Rabinovici, R. 2005. Torque ripple, vibrations, and acoustic noise in switched reluctance motors, HAIT Journal of Science and Engineering B, l. 2, 5-6, 776-786.

Schramm, D., Williams, B. W., and Green, T. C. 1992. Torque ripple reduction of switched reluctance motors by phase current optimal profiling, Proc. IEEE PESC"92, 1992, 857-860.

Sheth, N. K., and Rajagopal, K. R. 2003. Optimum pole arcs for a switched reluctance motor for higher torque with reduced ripple, IEEE Trans. Magn., 39(5), 3214-3216.

Sun, Z., Cheung, N. C., Pan, J., Zhao, S. W., and Gan, W.-C. 2008. Design and simulation of a magnetic levitated switched reluctance linear actuator system for high precision application, Proc. IEEE ISIE, 2, 624-629.

Zhao, S. W., Cheung, N. C., Gan, W.-C., Yang, J. M., and Pan, J. F. 2007. A self-tuning regulator for the high-precision position control of a linear switched reluctance motor, IEEE Trans. Ind. Electron., 54(5), 2425-2434.

Nomenclature

w_{sp}	width of the stator pole	(m)
w_{ss}	width of the stator slot	(m)
w_{sy}	stator back iron thickness	(m)
h_{sp}	stator pole height	(m)
w_{tp}	width of the translator pole	(m)
w_{ts}	width of the translator slot	(m)
w_{ty}	translator back iron thickness	(m)
h_{tp}	translator pole height	(m)
l_g	air gap length	(m)
V_{rated}	rated voltage	(V)
I_{rated}	rated current	(A)
V	velocity	(m/s)
F_{max}	maximum force	(N)
F_{min}	minimum force	(N)
F_{avg}	average force	(N)
F_L	load force	(N)
P_m	mechanical power output	(W)
N_{ph}	No. of turns per phase	
L_{stack}	stack length	(m)
L_{min}	minimum inductance	(H)
L_{max}	maximum inductance	(H)